

Evaluation of 10MeV Proton Irradiation on 5.5 Mpixel Scientific CMOS Image Sensor

Paul Vu, Boyd Fowler, Brian Rodricks, Janusz Balicki, Steve Mims, Wang Li
Fairchild Imaging
1801 McCarthy Blvd., Milpitas, CA 95035, USA

ABSTRACT

We evaluate the effects of 10 MeV proton irradiation on the performance of a 5.5 Mpixel scientific grade CMOS image sensor based on a 5T pixel architecture with pinned photodiode and transfer gate. The sensor has on-chip dual column level amplifiers and 11-bit single slope analog to digital converters (ADC) for high speed readout and wide dynamic range. The operation of the sensor is programmable and controlled by on-chip digital control modules. Since the image sensor features two identical halves capable of operating independently, we used a mask to expose only one half of the sensor to the proton beam, leaving the other half intact to serve as a reference. In addition, the pixel array and the digital logic control section were irradiated separately, at dose rates varying from 4 rad/s to 367 rad/s, for a total accumulated dose of 146 krad(Si) to assess the radiation effects on these key components of the image sensor. We report the resulting damage effects on the performance of the sensor including increase in dark current, temporal noise, dark spikes, transient effects and latch-up. The dark signal increased by about 55 e-/pixel after exposure to 14 krad (Si) and the dark noise increased from about 2.75e- to 6.5e-. While the number of hot pixels increased by 6 percent and the dark signal non uniformity degraded, no catastrophic failure mechanisms were observed during the tests, and the sensor did not suffer from functional failures.

Keywords: CMOS image sensor, Radiation Hardened by Design, Total Ionizing Dose, Displacement Damage, 10MeV Proton Irradiation, Single Event Effects,

1. INTRODUCTION

To support the design of a new high performance CMOS image sensor intended for earth observation applications, we performed 10 MeV proton irradiation tests on one of our existing imagers: a 5.5 Mpixel scientific grade CMOS image sensor, in order to assess the impact of displacement damage on the performance of the device and determine appropriate design changes to improve the radiation tolerance of the new design. The mission specifications require that the image sensor must be able to tolerate up to 13.5 krad(Si) total ionizing dose (TID). Although Co-60 is more commonly used to evaluate the impact of TID^[1], proton irradiation can be used to evaluate both displacement damage (DD) and TID effects. Since DD is typically not bias dependent, but TID is bias dependent and sensitive to dose rate, we performed our proton irradiation tests with the sensor fully operational at varying dose rates. Since the image sensor features two identical halves capable of operating independently, we placed an aperture mask at the proton beam exit window and positioned the beam to irradiate only one half of the sensor, leaving the other half of the device intact to serve as a reference. Furthermore, the pixel array, the column amplifiers, the ADC circuitry, and the digital logic control section were irradiated separately to assess the sensitivity of these key components of the image sensor to radiation exposure. While we do expect to observe a general increase in dark current^[2] and hot pixel density^[3] as a result of exposure to radiation, it was especially important for us to determine whether the readout circuitry and the digital control section of the device are susceptible to soft errors or latch-up failures so that suitable mitigation measures can be implemented.

2. TEST CONDITIONS

2.1 Sensor Overview

The image sensor used in this study is a Fairchild Imaging CIS2051^[4] with 2560(H) x 2160(V) 5T pixels with pinned photodiodes on a 6.5 μ m pixel pitch, fabricated in 0.18 μ m CMOS image sensor technology. The floorplan of the

CIS2051 is shown in Figure 1. The sensor consists of two independent halves. The pixel orientation is identical in both halves. The column amplifier circuits, ADCs and the digital control block (DCB) are located at the top and bottom of the array. The row control circuits are located on both sides of the pixel array.

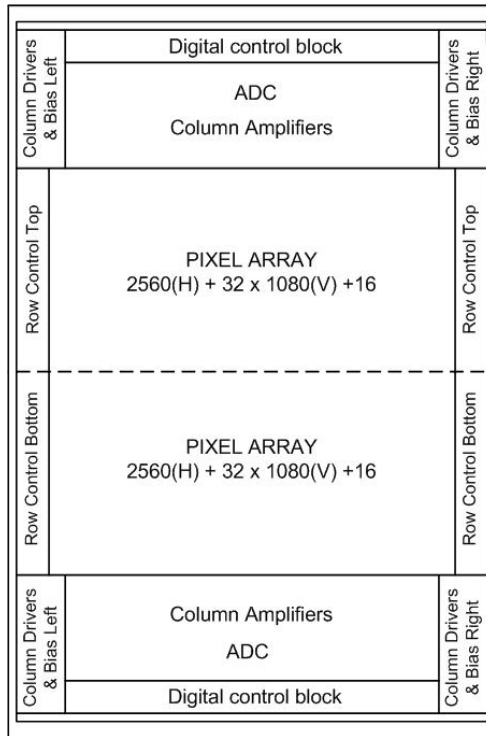


Figure 1. Floorplan of the Fairchild Imaging CIS2051 image sensor

Figure 2 shows a simplified schematic of the 5T pinned photodiode pixel. The charge transfer transistor connected to “TX1” is used to transfer charge from the pinned photodiode to the floating diffusion node. The reset transistor forces the floating diffusion node to “Vrst” when “Reset” is high. When “Word” is high the source follower is connected to the bit line and the voltage on the floating diffusion is read out. The transistor connected to “TX2” functions as a voltage controlled anti-blooming drain and serves as a global reset device.

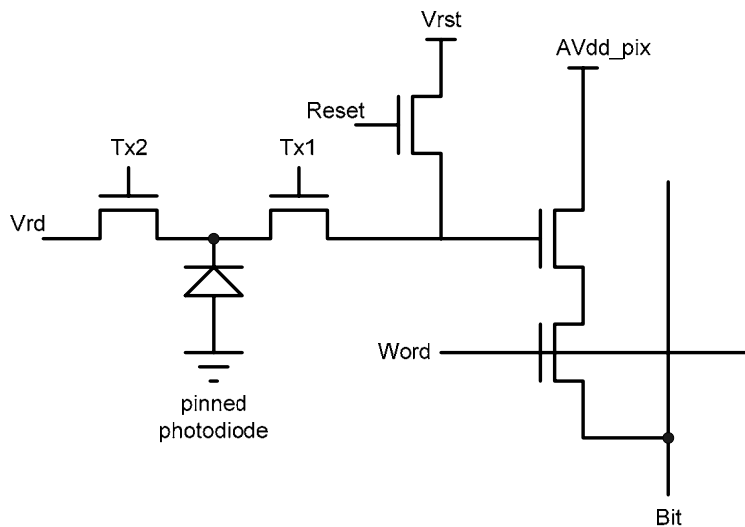


Figure 2. 5T pixel schematic

The sensor features on-chip dual column-level amplifiers and 11-bit single slope analog-to-digital converters (ADC). The dual column-level amplifier/ADC pairs have independent gain settings, and the final image is reconstructed by combining pixel output values from both the high- and low-gain readout channels to achieve a wide intra-scene dynamic range.

2.2. Test Conditions

The proton radiation tests were performed at the Crocker Nuclear Laboratory at UC Davis. Dosimetry was performed by the staff of Crocker Lab. The image sensor was mounted on a test development sensor control board and the sensor operation was remotely controlled and monitored from the control room next to the proton irradiation chamber. The test setup is shown below in Figure 3.

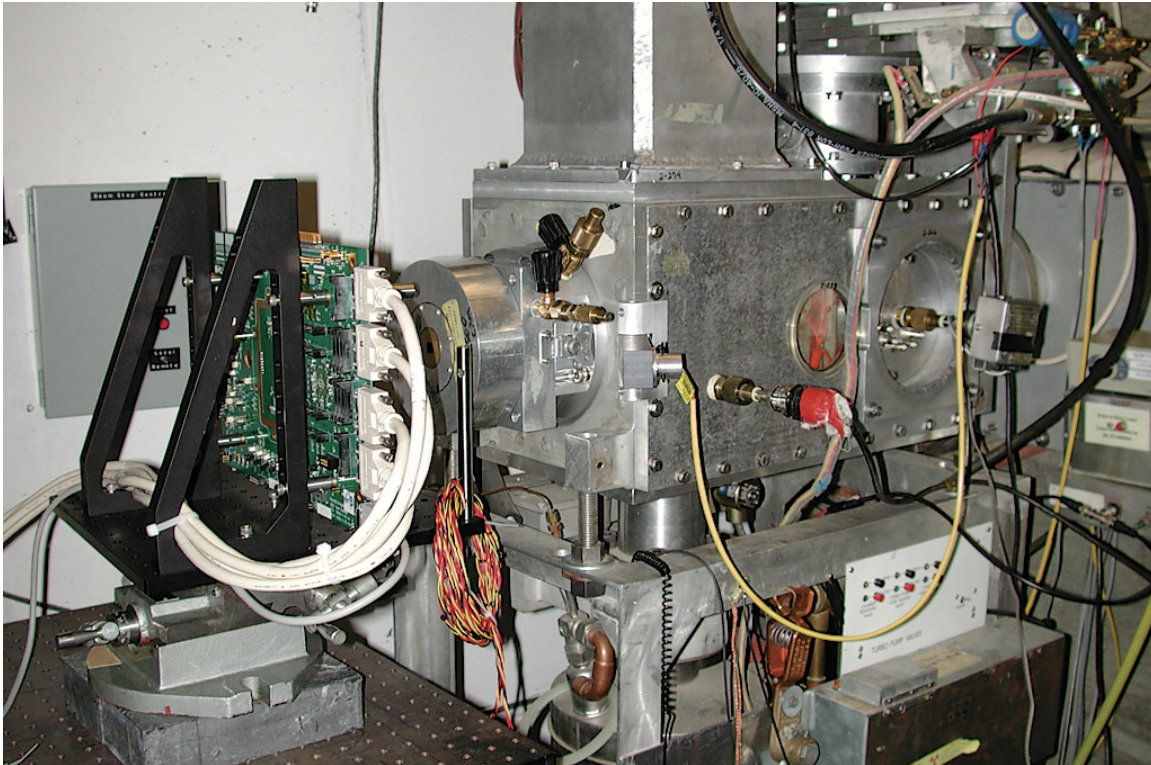


Figure 3. Proton test setup

A $1 \times 1 \text{ cm}^2$ aperture mask was inserted in the proton beam exit port to limit the region of exposure on the sensor. This setup is shown in Figure 4.

Selected regions of the image sensor were irradiated with 10 MeV protons at fluences of $2.4 \times 10^{10} \text{ p/cm}^2$ and $2.4 \times 10^{11} \text{ p/cm}^2$. Minimum TID was $\sim 13.5 \text{ krad(Si)}$ and $\sim 135.1 \text{ krad(Si)}$ respectively, and the total exposure time were approximately 63 min and 31 min at the two irradiation levels. The proton beam current was 40pA ($6.4 \times 10^6 \text{ p/cm}^2\text{-sec}$) and 800pA ($1.3 \times 10^7 \text{ p/cm}^2\text{-sec}$). Irradiation was performed at room temperature with the imager operating in standard imaging mode at 100MHz clock frequency. There was no lens attached to the image sensor, and the lights in the irradiation chamber were turned off during the irradiation tests.

The bottom half section of the active pixel array was subjected to irradiation first. At each exposure level, the beam was effectively blocked off every 10 minutes, and 40 image frames were captured in both low gain and high gain channels, and saved for off-line analysis. All image frames were collected at 33 ms integration time.

The column amplifier readout/ADC section and the digital control block (DCB) in the bottom half of the sensor were irradiated next, to monitor the device susceptibility to single event effects and latch-up. We monitored the current draw on the power supplies, and an image frame was saved every 30 seconds, including the DCB register settings. In addition, 40 image frames were collected at the end of every 10 minutes of irradiation time.

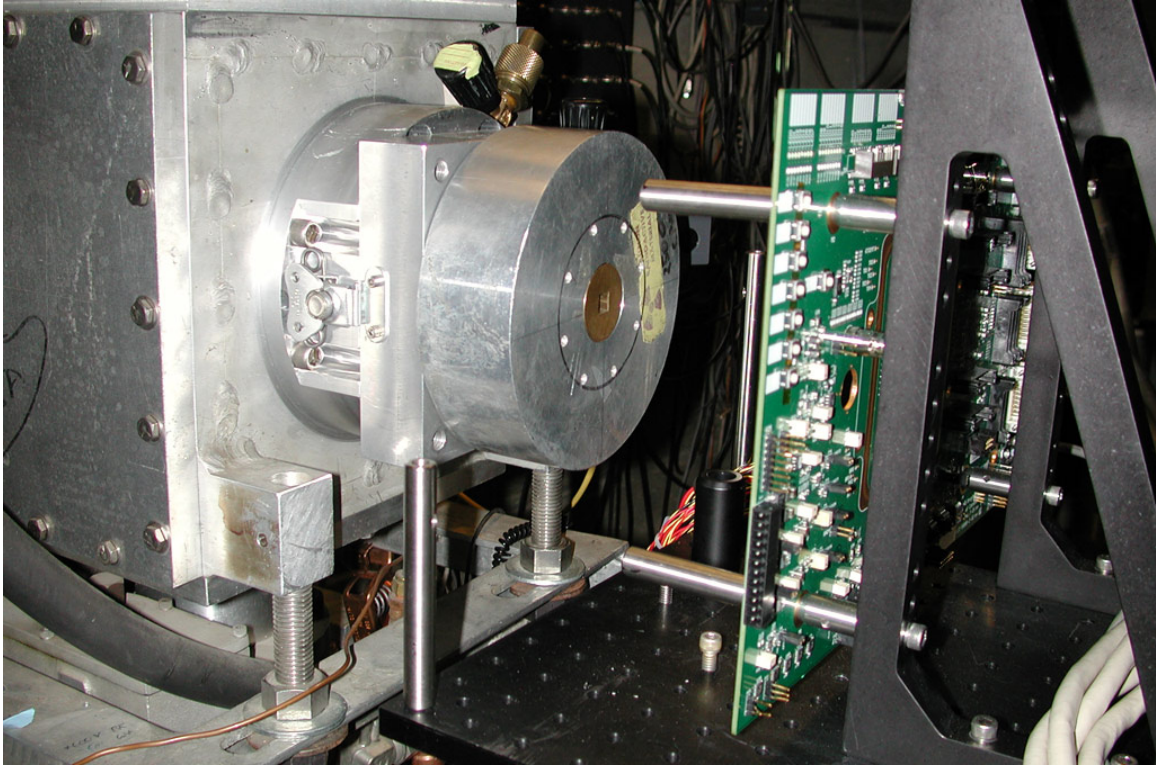


Figure 4. Proton beam aperture mask

3. RESULTS

3.1. Test Results and Observations

We analyzed the captured images and extract changes in dark signal, dark noise and hot pixel count. We define a hot pixel as one which dark signal amplitude is six standard deviations above the mean of the distribution. We compared the data measured in the irradiated section of the sensor against the data of the reference (unexposed) half of the sensor. The changes in dark signal and hot pixel count are plotted in Figure 5 and Figure 6.

Throughout the tests, the sensor functioned normally, and we did not observe any abnormal current increases or spikes in the power supplies and the DCB configuration register settings were stable indicating that single event effects (SEE) and single event latch-up (SEL) did not occur in this regime. The ADC operation did not show any anomalies, and no missing codes were observed in the collected image frames. The total noise in the high gain channel degraded from ~ 2.75 e-/pixel to ~ 6.5 e-/pixel due to the increase in dark current, the results are shown in Figure 7. The dark signal histograms, before and after irradiation, are shown in Figure 8. The image sensor normal operation was not interrupted during the tests, but the hot pixel density increased as a function of fluence, Figure 9 shows a dark frame histogram at 3.8×10^9 p/cm², 2 krad(Si), and Figure 10 shows a dark frame histogram at the end of the test when the total accumulated proton fluence reached 2.63×10^{11} p/cm², 146 krad(Si).

A decrease in sensitivity was observed in the region irradiated to 2.63×10^{11} p/cm², 146 krad(Si), and this condition did not change after storage at room temperature for two months.

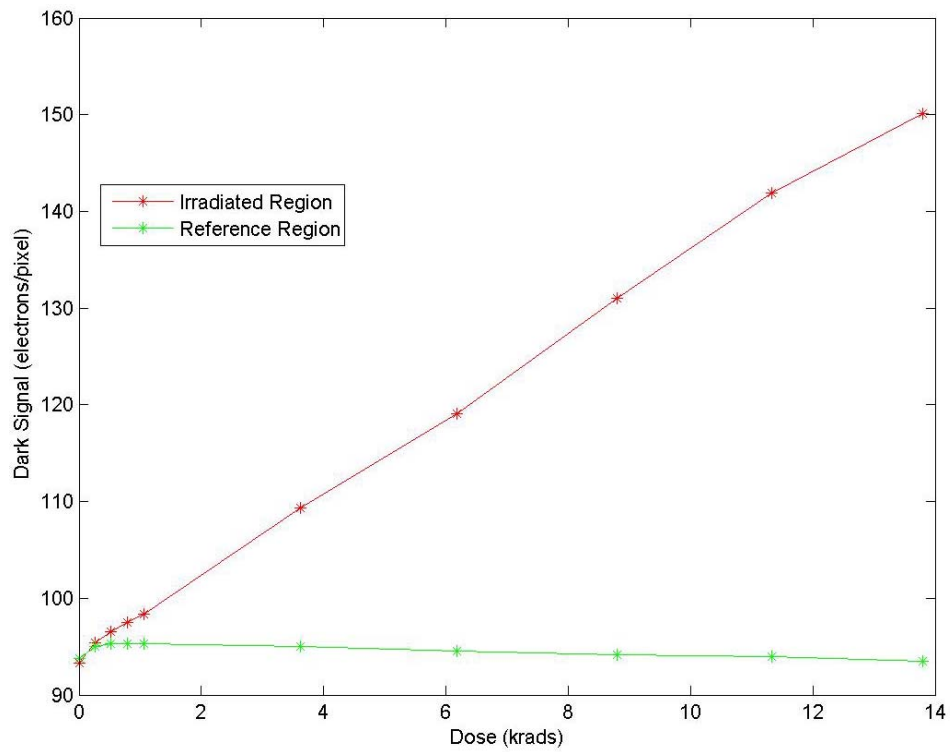


Figure 5. Increase in dark signal with total dose

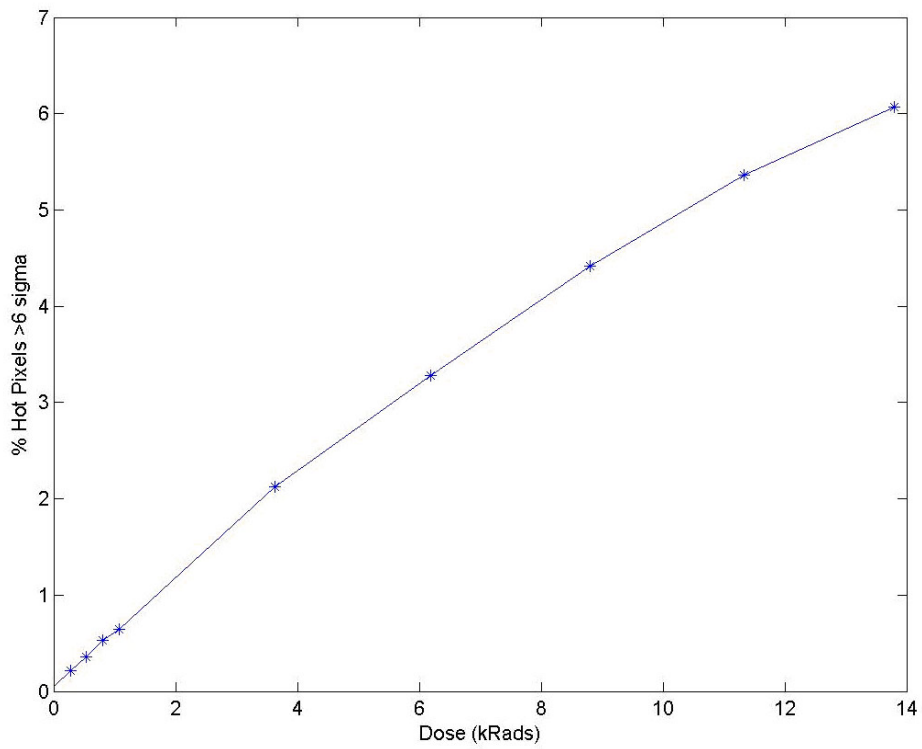


Figure 6. Increase in hot pixel density with total dose

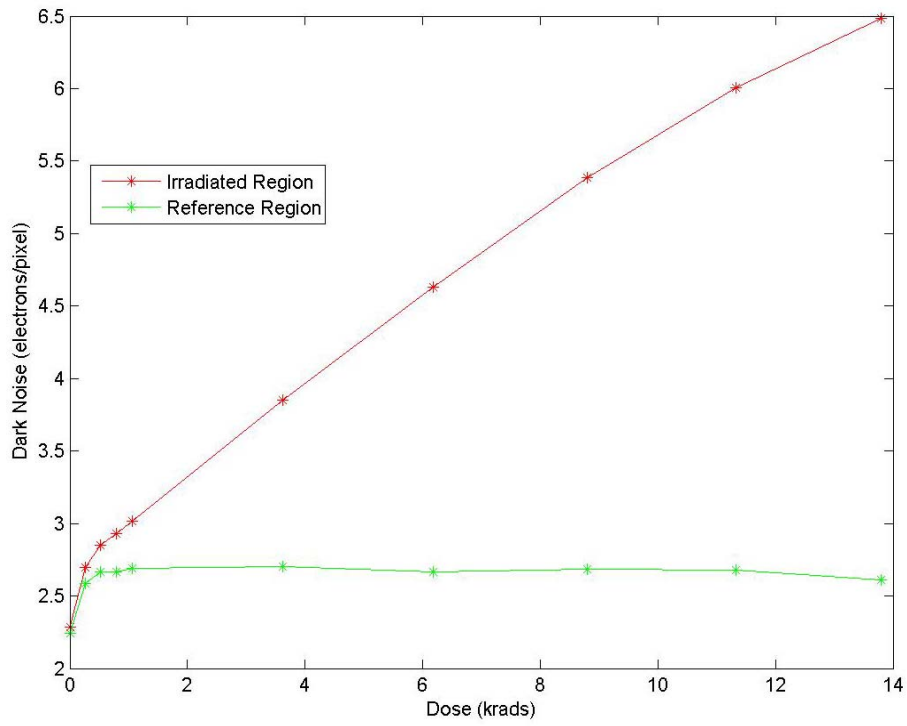


Figure 7. Total noise increase after irradiation due to higher dark current

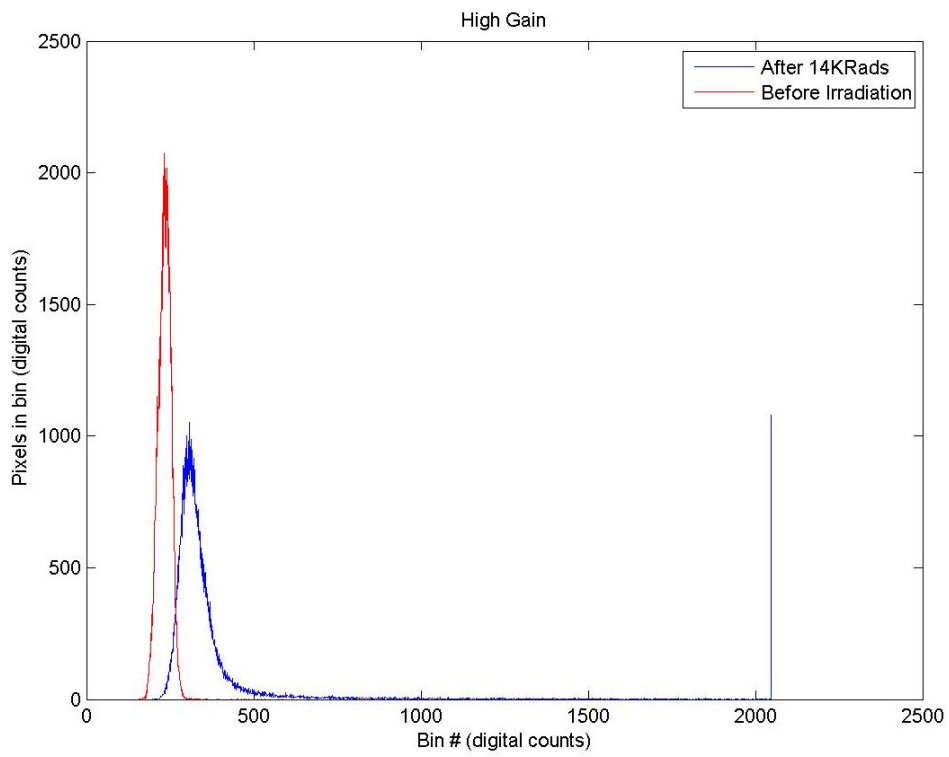


Figure 8. Dark signal histograms, before and after irradiation

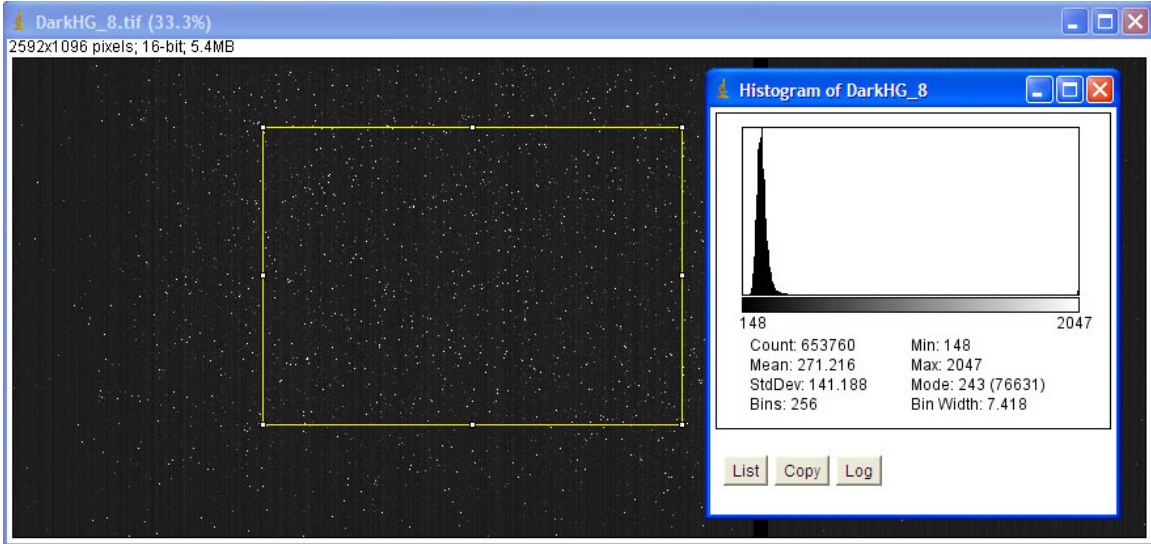


Figure 9. Image frame histogram at 3.8×10^9 p/cm², 2 krad(Si)

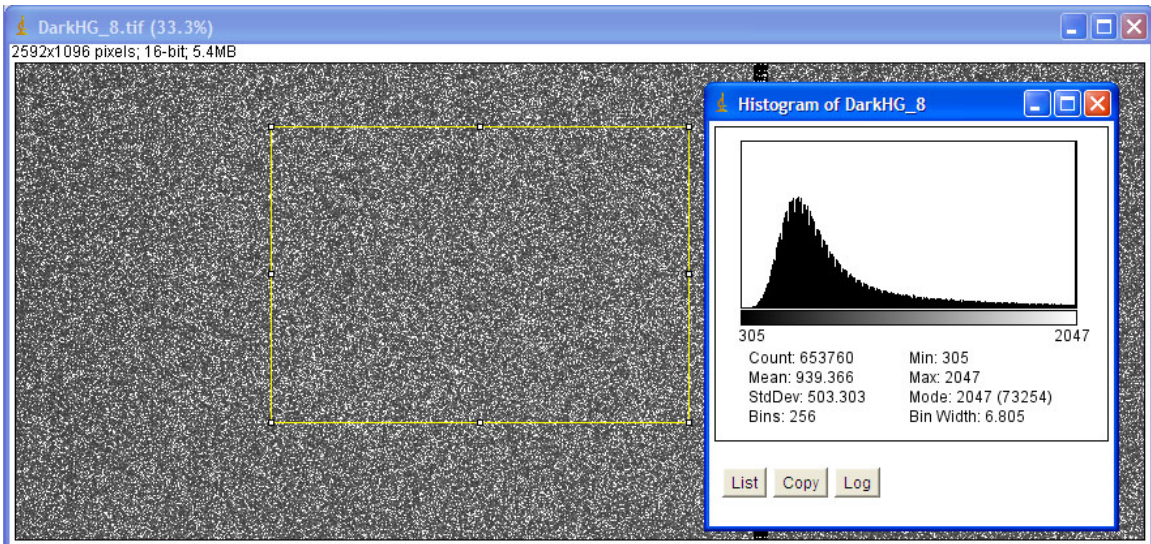


Figure 10. Image frame histogram at 2.63×10^{11} p/cm², 146 krad(Si)

3.2. Sensor Design Changes For Improved Radiation Tolerance

Although we did not encounter any catastrophic failures during the proton irradiation tests on a device that was not designed to be radiation tolerant, we are implementing the following changes in the design of a new sensor intended for space applications to improve its tolerance to radiation: p-channel and n-channel devices are enclosed with dedicated guard rings which effectively increases the distance between complementary devices, and a large number of additional substrate contacts and well contacts are placed at regular intervals. The changes in the layout of a transmission gate (TG) to improve the radiation tolerance of the device are shown in Figure 11, the changes significantly increase the size of the cell. Other precautions we have implemented to help minimize the increase in dark current due to leakage current in the pixels include increasing the separation between the n-photodiode region in the pixel from the shallow trench isolation (STI) structures.

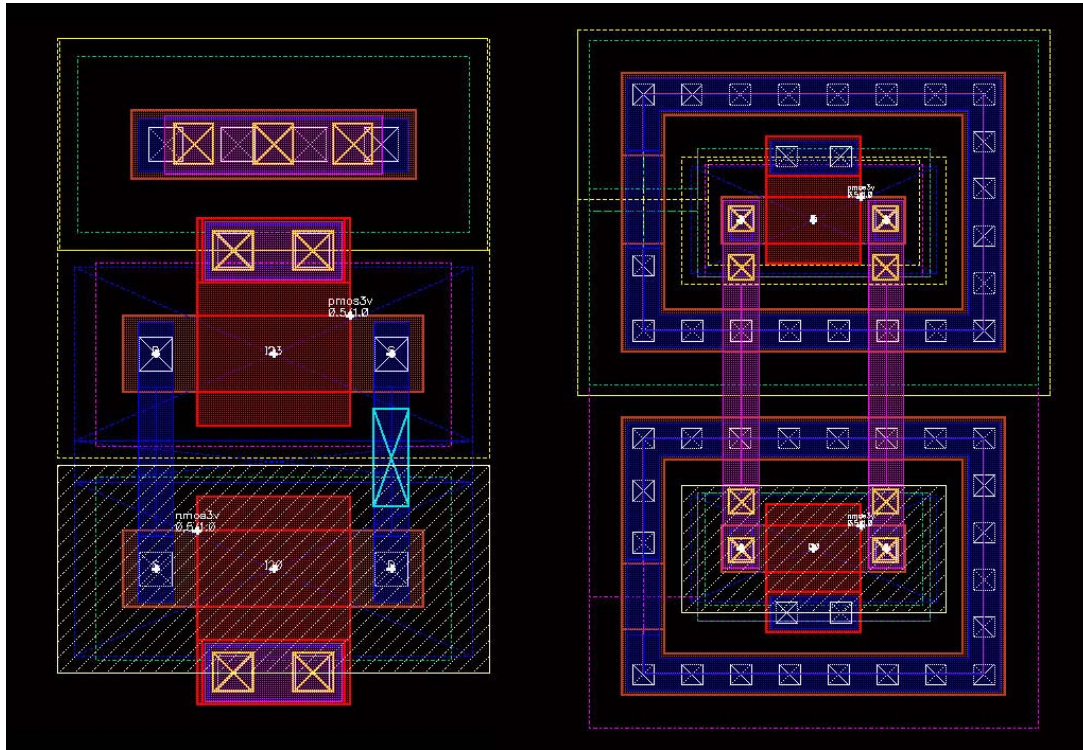


Figure 11. Layout of transmission gate: Standard (Left) vs. Radiation Tolerant (Right)

4. CONCLUSIONS

In an effort to evaluate the effects of radiation on the performance of a scientific grade CMOS image sensor designed with standard design techniques, we performed 10-MeV proton irradiation on the device at proton fluences of 2.4×10^{10} p/cm², 13.5 krad(Si) and 2.4×10^{11} p/cm², 135 krad(Si). The results of the tests indicate that the device survived 13.5 krad(Si), and the dominant degradation in sensor performance include: hot pixel formation, increase dark current, and reduction in sensitivity, but read noise did not degrade. While we did not experience any catastrophic failure modes, we have implemented a number of hardened-by-design (HBD) design techniques in a new sensor designed for space applications to improve the device tolerance to radiation. In addition, the design of the digital control block in the sensor was enhanced to accommodate periodic refresh of all register settings as a measure to mitigate against potential register corruption due to SEE incidents. The device will also feature a thinner epi layer which helps reduce the risk of latch-up caused by ionizing particles.

ACKNOWLEDGEMENTS

The authors would like to thank John Lowes, and Carlos Castenada (Crocker Nuclear Laboratory) for their valuable contributions and assistance in performing the proton irradiation tests.

REFERENCES

- [1] Goiffon, V., Etribeau, M., Magnan, P., "Overview of Ionizing Radiation Effects in Image Sensors Fabricated in a Deep-Submicrometer CMOS Imaging Technology", IEEE Transactions on Electron Devices, Vol. 56, No.11, Nov 2009
- [2] Bogaerts, J., Dierickx, B., Meynants, G., Uwaerts, D., "Total Dose and Displacement Damage Effects in a Radiation-Hardened CMOS APS", IEEE Transactions on Electron Devices, Vol 50, No. 1, Jan 2003
- [3] Scheick, S., Novak, F., "Hot Pixel Generation in Active Pixel Sensors: Dosimetric and Microdosimetric response", Radiation and its Effects on Component and Systems, Noorwijk, Netherlands, September, 2003
- [4] Fowler, B., Liu, C., Mims, S., Balicki, J., Li, W., Do, H., Appelbaum, J., Vu, P., "A 5.5Mpixel 100 Frames/sec Wide Dynamic Range Low Noise CMOS Image Sensor for Scientific Applications", Proc. of SPIE-IS&T Electronic Imaging, SPIE Vol. 7536, 2010